Trophoblast organoids with physiological polarity model placental structure and function

Liheng Yang[1], Pengfei Liang[2], Huanghe Yang[2,3] and Carolyn B. Coyne[1,4,5] *

[1]Department of Molecular Genetics and Microbiology, [2]Department of Biochemistry, [3]Department of Neurobiology, [4]Department of Immunology, [5]Duke Human Vaccine Institute, Duke University School of Medicine, Durham, NC, USA, Duke University Medical Center, Durham, NC, USA.

*Address correspondence:
Carolyn Coyne, PhD
3130 Medical Sciences Research Building III
3 Genome Court
Durham, NC 27710
USA
carolyn.coyne@duke.edu

ABSTRACT

Human trophoblast organoids (TOs) are a three-dimensional *ex vivo* culture model that can be used to study various aspects of placental development, physiology, and pathology. Previously, we showed that TOs could be derived and cultured from full-term human placental tissue and used as models of trophoblast innate immune signaling and teratogenic virus infections (Yang et al., 2022). However, a remaining challenge of TOs cultured in 'domes' of Matrigel or other extracellular matrix is their inverted polarity, with proliferative cytotrophoblasts (CTBs) on the outer surface of organoids and the multi-nucleated syncytiotrophoblast (STB) primarily localized within the inner surface, which is in direct contrast to the orientation that occurs *in vivo*. Here, we developed a method to culture TOs under conditions that recapitulate the cellular orientation of chorionic villi *in vivo*. We show that standard TOs containing the STB layer inside the organoid (STB^{in}) develop into organoids containing the STB on the outer surface (STB^{out}) when cultured in suspension with gentle agitation. STB^{out} organoids secrete higher levels of hormones and cytokines from the STB, including human chorionic gonadotropin (hCG) and interferon (IFN)-λ2. Using membrane capacitance measurements, we also show that the outermost surface of STB^{out} organoids contain large syncytia comprised of >60 nuclei compared to STB^{in} organoids that contain small syncytia (<6 nuclei) and mononuclear cells. The growth of TOs under conditions that mimic the cellular orientation of chorionic villi *in vivo* thus allows for the study of a variety of aspects of placental biology under physiological conditions.

INTRODUCTION

Three-dimensional organoid culture models from tissue-derived stem cells have emerged as important *ex vivo* systems to study a variety of aspects of the physiological and pathological states of their tissues of origin. Established organoid models often preserve key features of their source organs, including tissue organization and composition, expression signatures, immune responses, and secretion profiles. Importantly, organoid cultures can be propagated long-term and can often be cryopreserved, and thus have the capacity to serve as powerful *in vitro* tools even in the absence of access to new donor tissue. Over the past several years, trophoblast organoids (TOs) derived from human placentas at different gestational stages have emerged as models by which to study trophoblast development and biology, congenital infections, and innate immune defenses (Haider et al., 2018; Sheridan et al., 2020; Turco et al., 2018; Yang *et al.*, 2022). We have shown that TOs can be derived and cultured from full-term human placental tissue and used as models of trophoblast immunity and teratogenic pathogen infections (Yang *et al.*, 2022).

In most TO models, trophoblast stem/progenitor cells are isolated from placental chorionic villi by serial dissociation with digest solution followed by mechanical disruption (in the case of full-term tissue), then are then embedded within an extracellular matrix (ECM, such as Corning Matrigel or Cultrex BME) 'domes'. The domes containing isolated trophoblast stem/progenitor cells are then submerged in growth factor cocktail-reconstituted growth media to support stem/progenitor cell proliferation and differentiation as well as promoting their self-organization into mature organoid units. TOs differentiate to contain all trophoblast subtypes present in the human placenta, including proliferative cytotrophoblasts (CTBs), which differentiate into the multinucleated non-proliferative syncytiotrophoblast (STB), and invasive extravillous trophoblasts (EVTs). Human chorionic villi are covered by an outermost STB layer and an inner CTB layer that fuses to replenish the outer STB during pregnancy. However, TOs cultured as three-dimensional organoids embedded in ECM develop with the opposite polarity and mature organoids contain an inward-facing STB (STB^{in}) and an outward-facing CTB (Turco *et al.*, 2018; Yang *et al.*, 2022). This

59 inverse polarity limits the utility of TOs for studies that require access to the STB layer. For
60 example, STB^{in} TOs do not recapitulate the vertical transmission route of teratogenic infections,
61 the transport of nutrients and antibodies across the STB, or the release of hormones and other
62 factors that are critical for communication to maternal tissues and cells.

63 To overcome the limitation of existing TO models, we developed a suspension culture
64 method to reverse the polarity of TOs such that the STB layer is outward facing (STB^{out}). Similar
65 approaches have been developed and applied to a variety of epithelial-derived organoid models
66 (Co et al., 2019; Co et al., 2021; Kruger et al., 2020; Li et al., 2020; Salahudeen et al., 2020). We
67 show that this culture method not only reverses the polarity of STB^{in} TOs but enhances the
68 secretion of hormones and cytokines associated with the STB. Furthermore, we performed patch
69 clamping of STB^{in} and STB^{out} TOs to measure the size of cells comprising the outermost layer of
70 these organoids and found that STB^{out} organoids are covered by large syncytia, whereas STB^{in}
71 TOs contain smaller syncytia and are largely composed of mononuclear cells. The STB^{out} TO
72 culture model described here thus better reflects the physiological and pathological processes of
73 the human placenta, which can facilitate studies to define the underlying mechanisms of normal
74 and diseased placental conditions.

75

76 **MATERIALS AND METHODS**

77 **Trophoblast organoid culturing**

78 TO lines used in this study were derived as described previously (Yang *et al.*, 2022). For
79 passaging and culturing, TOs were plated into the Matrigel (Corning 356231) “domes”, then
80 submerged with prewarmed complete growth media as described (Yang *et al.*, 2022). Cultures
81 were maintained in a 37°C humidified incubator with 5% CO_2. Medium was renewed every 2-3
82 days. About 5-7 days after seeding TOs were collected from Matrigel “domes”, digested in
83 prewarmed TrypLE Express (Gibco, 12605-028) at 37°C for 8 min, then mechanically dissociated
84 into small fragments using an electronic automatic pipettor and further manually pipetting, if

85 necessary, followed by seeding into fresh Matrigel “domes” in 24-well tissue culture plates
86 (Corning 3526). Propagation was performed at 1:3-6 splitting ratio once every 5-7 days. For the
87 first 4 days after re-seeding, the complete growth media was supplemented with additional 5 μM
88 Y-27632 (Sigma, Y0503).
89

90 **Derivation of STB^{out} TOs by suspension culturing**

91 To generate STB^{out} TOs, mature STB^{in} organoids cultured as described above were first released
92 from Matrigel domes using cell recovery solution (Corning, 354253) on ice with constant rotating
93 at high speed (>120 rpm) for 30~60 min, pelleted, washed one time with basal media (Advanced
94 DMEM/F12 + 1% P/S + 1% L-glutamine + 1% HEPES) and resuspended in complete growth
95 media supplemented with additional 5 μM Y-27632. Organoids were then carefully transferred
96 using FBS pre-coated wide orifice p200 pipette tips (Fisher Scientific, 02-707-134) into an ultra-
97 low attachment 24-well plate (Corning, 3473). One dome containing ~ 500 organoids units can
98 be dispensed into up to 5 wells of a 24-well plate with < 100 organoids units per well. TOs were
99 evenly distributed in the wells prior to culturing in a 5% CO2 37℃ incubator for suspension culture
100 of 1-2 d. Constant orbital rotating can be introduced into suspension culture to improve polarity
101 reversal efficiency (Thermo Fisher, 88881103). Media was renewed daily, and any aggregates
102 dissociated using a FBS pre-coated wide orifice p200 pipette tip.
103

104 **Collection of conditioned media**

105 Conditioned media (CM) was collected from original STB^{in} in domes as described (Yang *et al.*,
106 2022). To harvest CM from STB^{out} TOs in suspension culture, the suspension culture 24-well plate
107 was tilted for ~2 min to sediment organoids to one side of the well, then carefully aspirate the
108 supernatant media without disturbing the bottom organoids. CM between STB^{in} and STB^{out} TOs
109 was the equivalent volume and contained approximately the same number of organoids per
110 sample.

111

112 **Immunofluorescence microscopy**

113 STB^{in} TOs were immunostained as was performed as described(Yang *et al.*, 2022). For staining
114 of STB^{out} TOs in suspension, the same protocol described was used, but the releasing of
115 organoids from Matrigel was omitted. The following antibodies or reagents were used: SDC-1
116 (Abcam, ab128936), cytokeratin-19 (Abcam, ab9221), Alexa Fluor 633-conjugated phalloidin
117 (Invitrogen, A22284), Alexa Fluor 594 Goat anti-Mouse IgG secondary antibody (Invitrogen,
118 A11032), Alexa Fluor 488 Goat anti-Rabbit IgG secondary antibody (Invitrogen, A11034). Images
119 were captured using a Zeiss 880 Airyscan Fast Inverted confocal microscope and contrast-
120 adjusted in Photoshop or Fiji. Image analysis was performed using Imaris (version 9.2.1, Oxford
121 Instruments).

122

123 **Luminex assays**

124 Luminex assays were performed using the following kits according to the manufacturer's
125 instructions: hCG Human ProcartaPlex Simplex Kit (Invitrogen, EPX010-12388-901), Bio-Plex
126 Pro Human Inflammation Panel 1 IL-28A / IFN-λ2 (Bio-rad, 171BL022M), Bio-Plex Pro Human
127 MMP-2 Set (Bio-rad, 171BL029M), Bio-Plex Pro Human Inflammation Panel 1, 37-Plex (Bio-rad,
128 171AL001M), and Bio-Plex Pro Human Chemokine Panel, 40-Plex (Bio-rad, 171AK99MR2).
129 Plates were washed using the Bio-Plex wash station (Bio-rad, 30034376) and read on a Bio-Plex
130 200 system (Bio-rad, 171000205). All samples from both polarity conditions (STB^{in} and STB^{out})
131 were tested in duplicate, and each condition was performed with at least three biological replicates.

132

133 **Coat-seeding of STB^{in} and STB^{out} TOs onto round coverslips for patch clamp**

134 To seed collected original STB^{in} TOs onto the round glass coverslips (VWR, 76305-514) pre-
135 coated with thin layer of Matrigel (Corning, 356231), each round coverslip was evenly distributed
136 with ~ 40 µl of Matrigel and carefully transferred into each well of regular 24-well plate to

137 polymerize in a 37 ℃ incubator for ~ 20 min. Then, organoids were harvested as described above
138 and evenly dispensed onto the Matrigel pre-coated surface of coverslips to settle down in a 5%
139 CO2 37 ℃incubator for 3~4 h to ensure that the majority of organoids attach onto the matrix
140 coating of the coverslip. For the STB^{out} TOs coat-seeding, the same protocol described above
141 was used except omitting the release of organoids from Matrigel domes.
142

143 **Patch clamp estimation of cell surface area**

144 All results were recorded in whole-cell configurations using an Axopatch 200B amplifier
145 (Molecular Devices) and the pClamp 10 software package (Molecular Devices). The glass
146 pipettes were pulled from borosilicate capillaries (Sutter Instruments) and fire-polished using a
147 microforge (Narishge) to reach a resistance of 2–3 MΩ. The pipette solution (internal) contained
148 (in mM): 140 CsCl, 1 $MgCl_2$, 10 HEPES, 0.2 EGTA. pH was adjusted to 7.2 by CsOH. The bath
149 solution contained (in mM): 140 CsCl, 10 HEPES, 1 $MgCl_2$. pH was adjusted to 7.4 by CsOH. All
150 experiments were at room temperature (22–25°C). All the chemicals for solution preparation were
151 obtained from Sigma-Aldrich. Once the whole cell configuration was established, a 10-mV voltage
152 command was delivered to the cell from a holding potential of 0 mV. The corresponding capacitive
153 current was recorded. Membrane capacitance of the cell was calculated using Clampfit software
154 (Molecular Devices) based on the following equation, $C_m = \frac{Q}{\Delta V} = \frac{I \times \Delta t}{\Delta V}$, where Cm is the membrane
155 capacitance, Q is the stored charge across the cell membrane, V is membrane voltage, I is current,
156 and t is time. For the histogram plot, the bins (x-axis) were set as (pF): 0-20, 20-100, 100-200,
157 200-500, 500-1000, 1000-2000, 2000-5000 and 5000-10000. The bars on the histogram were set
158 in the middle of each bin.
159

160 **Statistics and reproducibility**

161 All experiments reported in this study have been reproduced using independent organoids lines.
162 All statistical analyses were performed using Clampfit (Molecular Devices), Excel and Prism
163 software (GraphPad Software). Data are presented as mean ± SD, unless otherwise stated.
164 Statistical significance was determined as described in the figure legends. Parametric tests were
165 applied when data were distributed normally based on D'Agostino-Pearson analyses; otherwise,
166 nonparametric tests were applied. For all statistical tests, p value <0.05 was considered
167 statistically significant, with specific p values noted in the figure legends.
168

169 **RESULTS**

170 **Culturing of STB^{out} trophoblast organoids**

171 Like TOs, epithelial-derived organoids such as those from the GI tract develop with an
172 inward facing apical surface when grown in ECM domes (Co *et al.*, 2019; Co *et al.*, 2021).
173 However, this polarity can be reversed by culturing of differentiated organoids under suspension
174 culture conditions, which can occur within ~24 hrs of initiating these cultures (Co *et al.*, 2019; Co
175 *et al.*, 2021; Kruger *et al.*, 2020; Li *et al.*, 2020). Given this, we developed a TO culturing approach
176 that involves the culturing of organoids for 7 days in Matrigel domes to promote their formation
177 and differentiation, then the release of these organoids from Matrigel. Once released, organoids
178 were cultured for an additional period of 24-48 hrs in suspension with gentle agitation (schematic,
179 **Figure 1A**). Unlike epithelial organoids in which polarity reversal can be distinguished based on
180 brightfield microscopy alone (Co *et al.*, 2019; Co *et al.*, 2021), we were unable to clearly
181 distinguish between TOs grown in suspension (STB^{out}) and those cultured in Matrigel (STB^{in})
182 based on brightfield microscopy alone (**Figure 1B**). However, we did observe greater aggregation
183 of and/or fusion between organoids in STB^{out} TOs grown in suspension (**Figure 1C**). This
184 aggregation could be to avoided by limiting the number of organoids seeded into each well while
185 in suspension culture (to <100 organoids) and to disrupt aggregates by manual pipetting should
186 aggregation occur.

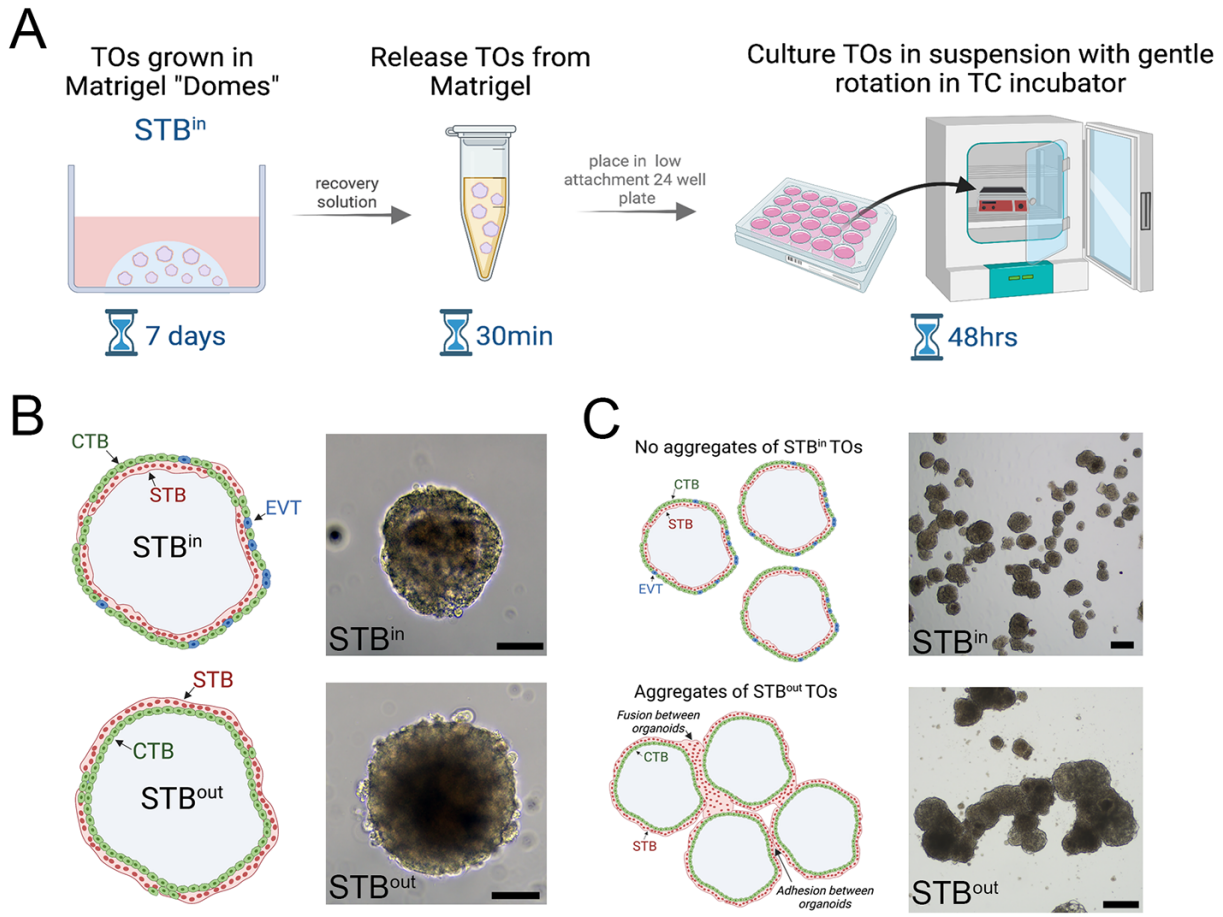

Figure 1: Development of STB^{out} trophoblast organoids. (A), Schematic of the protocol to generate STB^{out} trophoblast organoids (TOs) from STB^{in} TOs propagated in Matrigel domes. **(B),** Left, schematic of STB^{in} (top) or STB^{out} (bottom) TOs representing the cellular orientation of cytotrophoblasts (CTBs, in green), extravillous trophoblasts (in blue), and the syncytiotrophoblast (in red). Right, brightfield images of STB^{in} (top) or STB^{out} (bottom) TOs at the end of their culture period. Scale, 25μm. **(C),** Left, schematic of STB^{in} (top) or STB^{out} (bottom) TOs demonstrating the aggregation that can occurs in STB^{out} TOs that results from fusion of the STB between organoids and/or adhesion between organoids. At right, brightfield images of STB^{in} (top) or STB^{out} (bottom) TOs demonstrating the extent of aggregation that can occur. Scale, 150μm (top) and 125μm (bottom). All schematics created using Biorender.

To determine whether culturing of STB^{out} TOs in suspension led to alterations in the localization of the STB, we performed immuostaining for syndecan-1 (SDC-1), a cell surface proteoglycan that localizes to the apical surface of the STB, followed by three-dimensional confocal microscopy. In STB^{in} TOs cultured in Matrigel domes, most of the SDC-1 signal localized to the innermost surface of organoids (**Figure 2A, 2B**, **Supplemental Movie 1**). In contrast, SDC-

1 almost exclusively localized to the outermost surfaces of STB^{out} TOs (**Figure 2A**, **2B, Supplemental Movie 2**). This localization required culturing of TOs in suspension for ~48hrs as there was a significant increase in outer SDC-1 immunostaining in TOs cultured for 48hrs versus ~21hrs (**Figure 2C, 2D**).

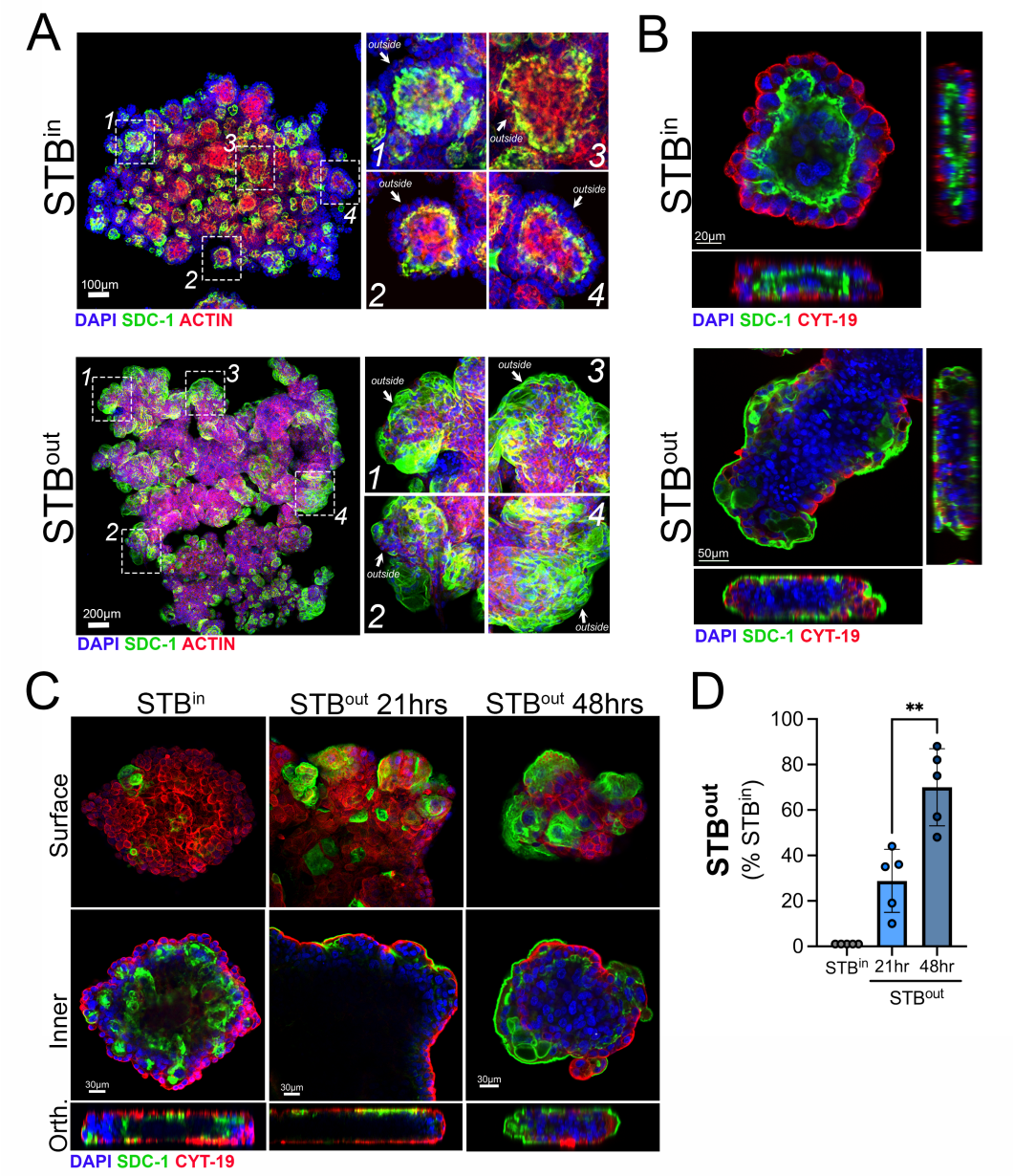

Figure 2: Confocal microscopy for the STB marker SDC-1 in STB^{in} and STB^{out} TOs. (A), Tile scanned confocal micrographs of STB^{in} (top) of STB^{out} (bottom) TOs immunostained for SDC-1 (green), and actin (red). DAPI-stained nuclei are in blue. Zoomed images of four fields shown in hatched white boxes are shown at right and the outside of the organoids shown by a white arrow.

(B), Cross sections of STB^{in} (top) of STB^{out} (bottom) TOs immunostained for SDC-1 (green), and cytokeratin-19 (red). DAPI-stained nuclei are in blue. At bottom and right are orthogonal views of three-dimensional stacked images. Movies demonstrating image reconstruction and sectioning are in Supplemental Movies 1 and 2. **(C),** Confocal micrographs of TOs cultured as STB^{in} (left panels) or in suspension to generate STBout for 21hrs (middle) or 48hrs (right) and immunostaining for SDC-1 (green) and cytokeratin-19 (red). DAPI-stained nuclei are in blue, Top panels were captured at the outermost surface of organoids (surface) and bottom panels were captured at the innermost layers (inner). Orthogonal views (Orth) are shown at bottom. **(D),** Image analysis of the extent of surface immunostaining for SDC-1 (shown as a percent of STB^{in} TOs) in STB^{out} TOs cultures for 21hrs (light blue) or 48hrs (dark blue). Data are shown as mean $\pm$ standard deviation with significance determined by a student's t-test (** $p<0.01$). Symbols represent unique fields of organoids from individual replicates.

Supplemental Movie 1: Three-dimensional image reconstruction of an STB^{in} trophoblast organoid (shown in Figure 2B, top) immunostained for SDC-1 (in green) and cytokeratin-19 (in red). DAPI-stained nuclei are shown in blue.

Supplemental Movie 2: Three-dimensional image reconstruction of an STB^{out} trophoblast organoid (shown in Figure 2B, bottom) immunostained for SDC-1 (in green) and cytokeratin-19 (in red). DAPI-stained nuclei are shown in blue.

STB-associated hormone and cytokine secretion is enhanced in STB^{out} organoids

The STB is a primary producer of hormones required for pregnancy, including human chorionic gonadotropin (hCG). We and others have shown that STB^{in} TOs recapitulate this secretion (Turco *et al.*, 2018; Yang *et al.*, 2022). To determine if there were differences in the secretion of hCG between STB^{in} and STB^{out} TOs, we performed Luminex assay from conditioned medium from these culture conditions. We found that there were significantly higher levels of hCG in media collected from STB^{out} TOs compared to STB^{in} TOs (~1500ng/mL versus ~220ng/mL, respectively).

In addition to hormones, the STB also secretes cytokines required to facilitate the establishment of tolerance and/or to defend the fetus from infection, such as the release of the antiviral type III interferons (IFNs) IFN-λs (Bayer et al., 2016). We showed previously that TOs

recapitulate this secretion and release a number of these cytokines, including IL-6 and IFN-λ2 (Yang *et al.*, 2022). To determine if STB^{out} TOs maintain this cytokine secretion or induce unique cytokines and chemokines compared to STB^{in} TOs, we performed multiplex Luminex profiling of >70 cytokines and chemokines, a subset of which we previously showed were released from STB^{in} TOs (Yang *et al.*, 2022). We did not observe any secretion of cytokines and chemokines in STB^{out} TOs that were not also secreted from STB^{in} TOs (**Figure 3B**). However, we found that STB^{out} TOs secreted higher levels of three factors, IFN-λ2 (55-fold increase), IL-6 (5.6-fold increase), and IL-6Ra (5.1-fold increase), and lower levels of a factor, MMP-2 (0.12-fold decrease) (**Figure 3B-3F**).

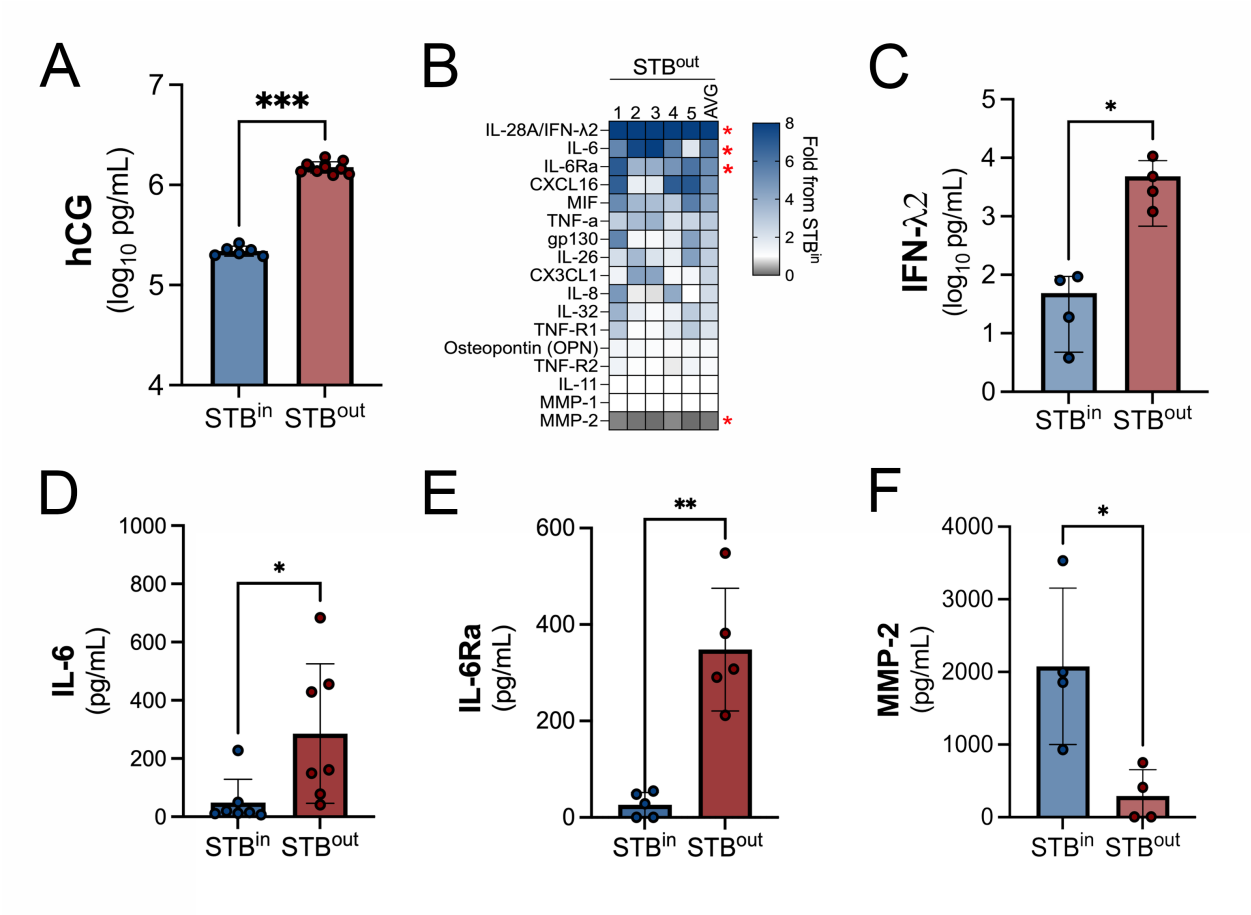

Figure 3: Levels of STB-associated hormones and cytokines in STB^{in} and STB^{out} TOs. (A), Levels of human chorionic gonadotropin (hCG) (shown as log_{10} pg/mL) in conditioned medium collected from STB^{in} or STB^{out} organoids as determined by Luminex. **(B),** Heatmap of cytokines and chemokines released from STB^{out} TOs. Data are shown as a fold-change from STB^{in} organoids (blue is increased and grey is decreased levels). Red asterisks designate factors

259 increased in STB^{out} TOs by >5-fold or decreased <1-fold. Data are shown from five independent
260 CM preparations with average shown at right. **(C-F),** Levels of IFN-λ2 (C) (shown as log_{10} pg/mL),
261 IL-6 (shown as pg/mL), IL-6Ra (shown as pg/mL), and MMP-2 (shown as pg/mL) in conditioned
262 medium collected from STB^{in} or STB^{out} organoids as determined by Luminex assays. In (A, C-F),
263 data are shown as mean ± standard deviation with significance determined by a student's t-test
264 (***, $p<0.001$, ** $p<0.01$, *$p<0.05$). Symbols represent unique media samples collected from
265 replicate experiments.
266

267 **Membrane capacitance measurements of STB^{out} TOs confirms the presence of large**
268 **syncytia on the outer organoid surface**

269 Cell fusion dramatically increases the surface area of the fused cell. As cell surface area
270 is proportional to its membrane capacitance (Cm) (Hodgkin and Huxley, 1952), patch clamp, a
271 quantitative electrophysiological technique (Gillis, 1995; Neher and Sakmann, 1976), can be used
272 to evaluate cell size. We therefore utilized patch clamping to calculate the size of cells/syncytia
273 comprising the exterior cellular surface of STB^{in} versus STB^{out} TOs (schematic, **Figure 4A**). When
274 a small voltage step (10 mV) was applied, the capacitive current from STB^{out} TOs showed much
275 slower decay than the capacitive current from STB^{in} TOs (**Figure 4D**). The average Cm in STB^{in}
276 versus STB^{out} TOs were 238.2 ±68 pF and 2,812.0 ± 381.8 pF, respectively (**Figure 4C**).
277 Interestingly, the Cm of the surface trophoblasts in STB^{out} TOs exhibits a Gaussian distribution
278 (**Figure 4E**). In stark contrast to the broader distribution of the Cm from STB^{in} TOs centered at
279 113.5 pF, the Cm from the STB^{out} TOs was largely centered at 3,349.6 pF, about 30-fold larger
280 than in STB^{in} TOs. It is worth noting that extremely large syncytia are readily observed on the
281 surfaces of STB^{out} TOs (**Figures 2C and S1A**). We recorded 5 independent areas of these cells
282 and found that they have unmeasurable cell capacitance (**Figure S1B**). This is likely due to space
283 clamp issues for syncytia with extremely large surface areas (Spruston et al., 1993). Based on
284 these observations, we conclude that the surface trophoblasts from STB^{in} TOs are mainly
285 composed of single-nucleated CTBs and syncytia with limited fusion (less than 10 nuclei). In
286 contrast, the surface trophoblasts from STB^{out} TOs primarily consisted of syncytia containing
287 greater than 60 nuclei.

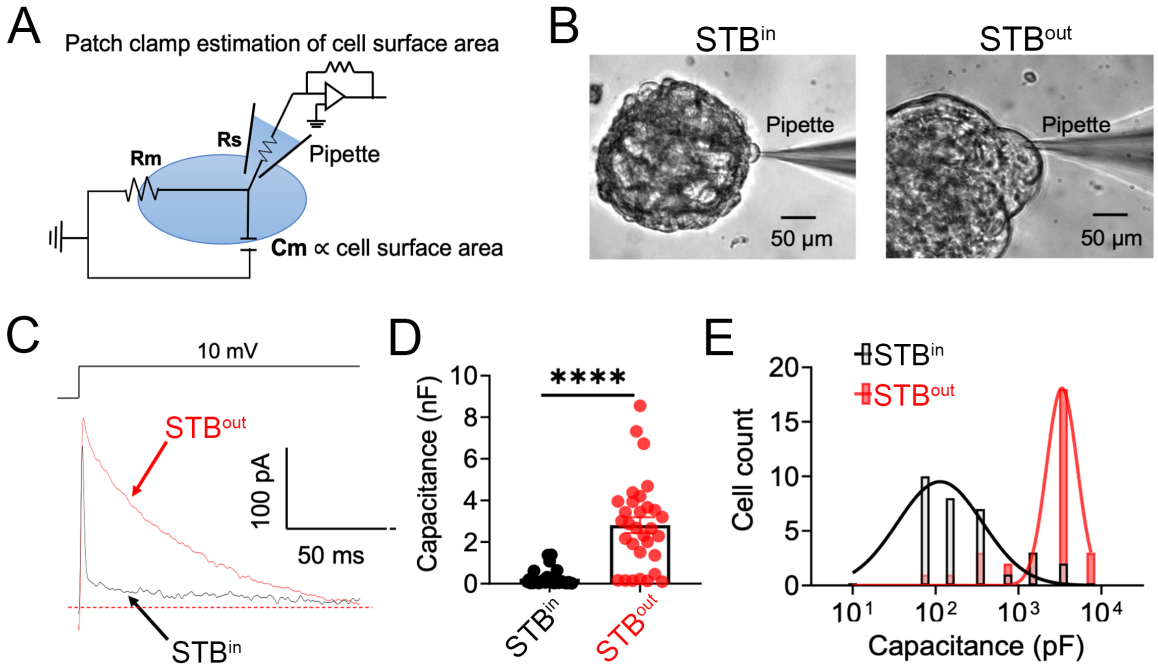

Figure 4: Evaluation of trophoblast fusion on the surface of STB^{in} and STB^{out} TOs using membrane capacitance measurement. (A), Diagram of whole-cell patch clamp to measure membrane capacitance (Cm), which is proportional to cell surface area. Rs: series resistance; Rm: membrane resistance. **(B),** Representative brightfield images of patch-clamped surface trophoblasts from the TOs growing under STB^{in} (left) or STB^{out} (right) conditions. **(C),** Representative membrane test traces from STB^{in} (black line) and STB^{out} (red line) TOs to measure cell capacitance. Current was elicited by a test voltage pulse of 10 mV from a holding potential of 0 mV (top). **(D),** Summary of membrane capacitance measured from STB^{in} (black) and STB^{out} (red) TOs. Two-sided Student's t-test, ****$p<0.0001$ (n=31 for each condition). **(E)** Distribution of cell capacitance from STB^{in} (black) and STB^{out} (red) TOs. The bars were at the center of each bin (see Methods for details). The data were fitted with Gaussian distribution.

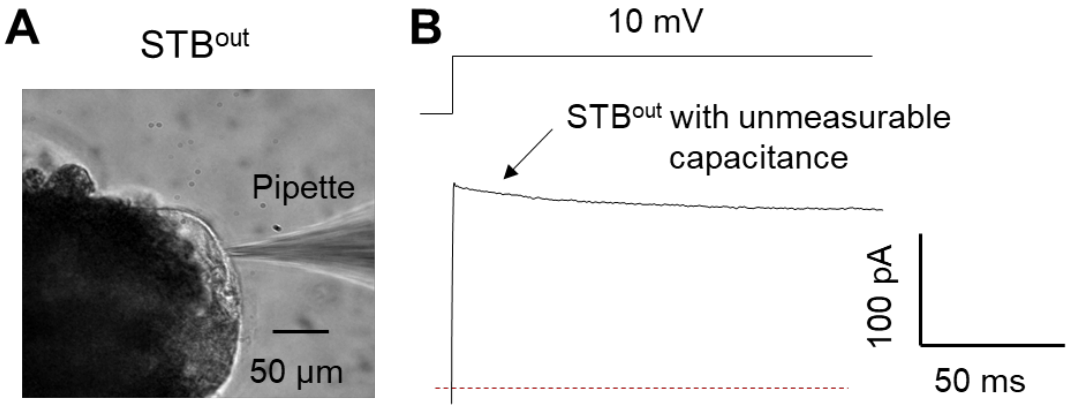

Figure S1. Patch clamp measurement of large syncytia from the surface of STB^{out} TOs. A), Representative brightfield image of a patch-clamped, extremely large syncytia from trophoblast

organoids (TOs) growing under STB^{out} conditions. **(B),** Representative membrane test trace from large STB. Cell capacitance cannot be accurately measured due to the space clamp issue of large syncytia. Current was elicited by a test voltage pulse of 10 mV from a holding potential of 0 mV (top).

DISCUSSION

In this study, we developed a method to culture trophoblast organoids under conditions that better reflect their cellular orientation *in vivo*. This model facilitates access to the STB layer while also maintaining key features associated with STB^{in} TOs, including their three-dimensional morphology, the presence of multiple trophoblast subpopulations, and the secretion of pregnancy related hormones and immune factors. STB^{out} TOs have several advantages over STB^{in} TOs. For example, STB^{out} TOs naturally self-reorganize with an STB outward-facing surface and do not require extensive manipulation to develop an outer STB layer. In addition, given that the STB localizes to the outer layer, STB^{out} TOs produce higher levels of hormones, cytokines, and possibly other factors secreted by the STB. Lastly, as STB^{out} TOs are cultured in suspension, the lack of ECM allows for applications in which this scaffold presents a barrier to diffusion, such as studies of microbial infections or antibody uptake.

For epithelial organoids grown in ECM domes with basal-out polarity, microinjection can serve as an option to directly access the enclosed apical surface (Bartfeld et al., 2015; Bartfeld and Clevers, 2015). However, in contrast to epithelial-derived organoid types which often form clear cystic structures, TOs have dense/solid structures, which makes microinjection of these organoids difficult. Additional methods have been applied to epithelial-derived organoids, such as seeding the dissociated organoid fragments onto Transwell inserts (Good et al., 2019; VanDussen et al., 2015). However, this approach comprises the three-dimensional nature of organoids which impacts their function. The method we describe here avoids several of the challenges described above as STB^{out} TOs maintain their three-dimensional structure and do not require their disruption to generate. It is unclear whether STB^{in} TOs undergo similar mechanisms of polarity reversal as do epithelial-derived organoids, which undergo relocalization of junction-associated proteins to

332 mediate this process, or whether culturing in suspension instead promotes CTB fusion on the
333 organoid surface. Given that the surface of STB^{out} TOs are covered by very large syncytia, it is
334 possible that suspension culturing promotes the fusion of CTBs on the organoid surface rather
335 than inducing a relocalization of the STB from the inner to outer organoid surface.

336 A benefit of TOs is their ability to recapitulate the hormone and cytokine secretion
337 observed in primary trophoblasts and chorionic villous tissue explants (Yang *et al.*, 2022), which
338 is not recapitulated in standard trophoblast cell lines (Bayer *et al.*, 2016). However, given that
339 STB^{in} TOs are embedded in Matrigel, many of these STB-associated factors would be secreted
340 into the center of the organoid structure or perhaps into the surrounding ECM. We found that
341 STB^{out} TOs not only recapitulate the release of these factors but were secreted at significantly
342 higher levels than those observed in STB^{in} TOs. The mechanistic basis for this is likely two-fold
343 and could include the increase in syncytia size on the STB^{out} TO surface as well as the direct
344 release of these factors into the culture media. However, it should be noted that we observed a
345 significant reduction in the release of MMP-2, which is specifically released from EVTs. This
346 finding suggests that there may be reduced EVT differentiation in STB^{out} TOs that likely results
347 from the lack of ECM. It is not clear whether methods to promote EVT differentiation previously
348 applied to TOs derived from full-term tissue (Yang *et al.*, 2022) could also be applied to the STB^{out}
349 TO system. However, given the extended time to perform this procedure (>3 weeks), it is unlikely
350 that STB^{out} TOs would be amenable to this process.

351 STB^{out} TOs contain a large population of syncytia formed by the fusion of CTBs. Here, we
352 leveraged the power of electrophysiology to define the size of syncytia covering the surface of
353 STB^{in} and STB^{out} TOs. These studies verified the high efficiency of the STB^{out} TO system and
354 provided quantitative measurements of the number of nuclei comprising syncytia. These studies
355 estimated that syncytia covering STB^{out} TOs were comprised of at least 60 nuclei as well as some
356 syncytia that were too large to be measured by patch clamping. These studies not only confirmed

357 the presence of syncytia on the outer surface of STB^{out} TOs but provide a strong proof of concept
358 for the application of this approach to quantitatively measure syncytial size on the surfaces of TOs,
359 which could be applied to a variety of biological questions.

360 The model described here provides an organoid system that recapitulates the cellular
361 orientation of the human placenta *in vivo* and provides evidence that this system can be used to
362 model key aspects of STB structure and function.

363

364 **RESOURCE AVAILABILITY**

365 **Lead contact**

366 Further information and requests for resources and reagents should be directed to and will be
367 fulfilled by the lead contact, Dr. Carolyn Coyne (carolyn.coyne@duke.edu)

368 **Materials availability**

369 All reagents generated in this study will be made available on reasonable request.

370 **Data and code availability**

371 The datasets supporting the current study are available from the corresponding author on request.

372

373 **ACKNOWLEDGMENTS**

374 This work was supported by the NIH grants R01AI145828 (C.B.C.) and DP2GM126898 (H.Y.).
375 We also gratefully acknowledge the Duke Light Microscopy Core Facility for their technical
376 support and assistance for this work.

377

378 **AUTHOR CONTRIBUTIONS**

379 L.Y. and C.C. conceived the study, developed the methodology, and analyzed the data; P.L. and
380 H.Y. performed patch clamping measurement, and analyzed the data; All authors participated in
381 manuscript writing, review, and editing.

DECLARATION OF INTERESTS

The authors declare no competing interests.

REFERENCES

Bartfeld, S., Bayram, T., van de Wetering, M., Huch, M., Begthel, H., Kujala, P., Vries, R., Peters, P.J., and Clevers, H. (2015). In vitro expansion of human gastric epithelial stem cells and their responses to bacterial infection. Gastroenterology *148*, 126-136 e126. 10.1053/j.gastro.2014.09.042.

Bartfeld, S., and Clevers, H. (2015). Organoids as Model for Infectious Diseases: Culture of Human and Murine Stomach Organoids and Microinjection of Helicobacter Pylori. J Vis Exp. 10.3791/53359.

Bayer, A., Lennemann, N.J., Ouyang, Y., Bramley, J.C., Morosky, S., Marques, E.T., Jr., Cherry, S., Sadovsky, Y., and Coyne, C.B. (2016). Type III Interferons Produced by Human Placental Trophoblasts Confer Protection against Zika Virus Infection. Cell Host Microbe *19*, 705-712. 10.1016/j.chom.2016.03.008.

Co, J.Y., Margalef-Catala, M., Li, X., Mah, A.T., Kuo, C.J., Monack, D.M., and Amieva, M.R. (2019). Controlling Epithelial Polarity: A Human Enteroid Model for Host-Pathogen Interactions. Cell Rep *26*, 2509-2520 e2504. 10.1016/j.celrep.2019.01.108.

Co, J.Y., Margalef-Catala, M., Monack, D.M., and Amieva, M.R. (2021). Controlling the polarity of human gastrointestinal organoids to investigate epithelial biology and infectious diseases. Nat Protoc *16*, 5171-5192. 10.1038/s41596-021-00607-0.

Gillis, K.D. (1995). Techniques for Membrane Capacitance Measurements. In Single-Channel Recording, B. Sakmann, and E. Neher, eds. (Springer US), pp. 155-198. 10.1007/978-1-4419-1229-9_7.

Good, C., Wells, A.I., and Coyne, C.B. (2019). Type III interferon signaling restricts enterovirus 71 infection of goblet cells. Sci Adv *5*, eaau4255. 10.1126/sciadv.aau4255.

Haider, S., Meinhardt, G., Saleh, L., Kunihs, V., Gamperl, M., Kaindl, U., Ellinger, A., Burkard, T.R., Fiala, C., Pollheimer, J., et al. (2018). Self-Renewing Trophoblast Organoids Recapitulate the Developmental Program of the Early Human Placenta. Stem Cell Reports *11*, 537-551. 10.1016/j.stemcr.2018.07.004.

Hodgkin, A.L., and Huxley, A.F. (1952). A quantitative description of membrane current and its application to conduction and excitation in nerve. The Journal of physiology *117*, 500-544.

Kruger, M., Oosterhoff, L.A., van Wolferen, M.E., Schiele, S.A., Walther, A., Geijsen, N., De Laporte, L., van der Laan, L.J.W., Kock, L.M., and Spee, B. (2020). Cellulose Nanofibril Hydrogel Promotes Hepatic Differentiation of Human Liver Organoids. Adv Healthc Mater *9*, e1901658. 10.1002/adhm.201901658.

Li, Y., Yang, N., Chen, J., Huang, X., Zhang, N., Yang, S., Liu, G., and Liu, G. (2020). Next-Generation Porcine Intestinal Organoids: an Apical-Out Organoid Model for Swine Enteric Virus Infection and Immune Response Investigations. J Virol *94*. 10.1128/JVI.01006-20.

Neher, E., and Sakmann, B. (1976). Single-channel currents recorded from membrane of denervated frog muscle fibres. Nature *260*, 799-802. 10.1038/260799a0.

470 Salahudeen, A.A., Choi, S.S., Rustagi, A., Zhu, J., van Unen, V., de la, O.S., Flynn, R.A.,
471 Margalef-Catala, M., Santos, A.J.M., Ju, J., et al. (2020). Progenitor identification and SARS-CoV-
472 2 infection in human distal lung organoids. Nature *588*, 670-675. 10.1038/s41586-020-3014-1.

473 Sheridan, M.A., Fernando, R.C., Gardner, L., Hollinshead, M.S., Burton, G.J., Moffett, A., and
474 Turco, M.Y. (2020). Establishment and differentiation of long-term trophoblast organoid cultures
475 from the human placenta. Nat Protoc *15*, 3441-3463. 10.1038/s41596-020-0381-x.

476 Spruston, N., Jaffe, D.B., Williams, S.H., and Johnston, D. (1993). Voltage- and space-clamp
477 errors associated with the measurement of electrotonically remote synaptic events. J
478 Neurophysiol *70*, 781-802. 10.1152/jn.1993.70.2.781.

479 Turco, M.Y., Gardner, L., Kay, R.G., Hamilton, R.S., Prater, M., Hollinshead, M.S., McWhinnie,
480 A., Esposito, L., Fernando, R., Skelton, H., et al. (2018). Trophoblast organoids as a model for
481 maternal-fetal interactions during human placentation. Nature *564*, 263-267. 10.1038/s41586-
482 018-0753-3.

483 VanDussen, K.L., Marinshaw, J.M., Shaikh, N., Miyoshi, H., Moon, C., Tarr, P.I., Ciorba, M.A.,
484 and Stappenbeck, T.S. (2015). Development of an enhanced human gastrointestinal epithelial
485 culture system to facilitate patient-based assays. Gut *64*, 911-920. 10.1136/gutjnl-2013-306651.

486 Yang, L., Semmes, E.C., Ovies, C., Megli, C., Permar, S., Gilner, J.B., and Coyne, C.B. (2022).
487 Innate immune signaling in trophoblast and decidua organoids defines differential antiviral
488 defenses at the maternal-fetal interface. Elife *11*. 10.7554/eLife.79794.
489